

Proceedings of the 16th Czech and Slovak Conference on Magnetism, Košice, Slovakia, June 13–17, 2016

Superconductivity in $\text{Lu}_x\text{Zr}_{1-x}\text{B}_{12}$ Dodecaborides with Cage-Glass Crystal Structure

N. SLUCHANKO^{a,b}, A. AZAREVICH^{a,*}, A. BOGACH^a, S. GAVRILKIN^c, V. GLUSHKOV^{a,b},
S. DEMISHEV^{a,b}, K. MITSSEN^c, N. SHITSEVALOVA^d, V. FILIPPOV^d, S. GABANI^e
AND K. FLACHBART^e

^aProkhorov General Physics Institute, RAS, Vavilov Str. 38, 119991 Moscow, Russia

^bMoscow Institute of Physics and Technology, Institutskii per. 9, 141700, Dolgoprudnyi, Russia

^cLebedev Physical Institute RAS, Leninskii av. 53, 119991 Moscow, Russia

^dFrantsevich Institute for Problems of Materials Science, NASU, Krzhizhanovskii Str. 3, 03680 Kiev, Ukraine

^eInstitute of Experimental Physics, SAS, Watsonova 47, 040 01 Košice, Slovakia

We probed the evolution of the superconducting transition temperature T_c and the normal state parameters of $\text{Lu}_x\text{Zr}_{1-x}\text{B}_{12}$ solid solutions employing resistivity, heat capacity and magnetization measurements. In these studies of high-quality single crystals it was found that there are two types of samples with different magnetic characteristics. An unusually strong suppression of superconductivity in $\text{Lu}_x\text{Zr}_{1-x}\text{B}_{12}$ with a rate $dT_c/dx = 0.21$ K/at.% of Lu was observed previously on the first “magnetic” set of crystals, and it was argued to be caused by the emergence of static spin polarization in the vicinity of non-magnetic lutetium ions. On the contrary, the second (current) set of “nonmagnetic” crystals demonstrates a conventional $T_c(x)$ dependence with a rate $dT_c/dx = 0.12$ K/at.% of Lu which is typical for BCS-type superconductors doped by nonmagnetic impurities. The reason for this difference is yet unclear. Moreover, the H – T phase diagram of the superconducting state of $\text{Lu}_x\text{Zr}_{1-x}\text{B}_{12}$ ($0 \leq x \leq 1$) solid solutions has been deduced from magnetization measurements.

DOI: [10.12693/APhysPolA.131.1036](https://doi.org/10.12693/APhysPolA.131.1036)

PACS/topics: 74.25.-q, 74.62.Bf, 74.70.Ad

1. Introduction

The discovery of superconductivity at $T_c \approx 39$ K in MgB_2 [1] has stimulated a significant interest into studies of a wide class of rare-earth and transition metal higher borides. Among them, in the family of dodecaborides, ZrB_{12} is a BCS (Bardeen-Cooper-Schriffer) superconductor with the highest $T_c \approx 6$ K [2, 3]. However, in case of LuB_{12} the superconducting transition temperature reduces dramatically ($T_c \approx 0.4$ K for LuB_{12} [4–6]), and the origin of the large T_c difference for these two compounds with similar conduction bands and crystalline structures is not yet clarified. In this connection the study of normal state characteristics of $\text{Lu}_x\text{Zr}_{1-x}\text{B}_{12}$ solid solutions with $x < 0.08$ at low temperatures allowed to observe the formation of static nanosized magnetic moments with $\mu_{\text{eff}} \approx 6\mu_B$ per Lu^{3+} ion (1S_0 ground state, $4f^{14}$ -configuration) in the vicinity of nonmagnetic lutetium impurities in the nonmagnetic Zr-rich matrix [7]. According to arguments presented in [7], the strong suppression of superconductivity in $\text{Lu}_x\text{Zr}_{1-x}\text{B}_{12}$ compounds can be attributed to pair breaking arising in the vicinity of these nanosized lutetium magnetic domains. In order to shed more light on the nature of the T_c variation in these dodecaborides it looks promising to investigate the normal

and superconducting states’ parameters of $\text{Lu}_x\text{Zr}_{1-x}\text{B}_{12}$ solid solutions in a wide range of Lu content ($0 \leq x \leq 1$).

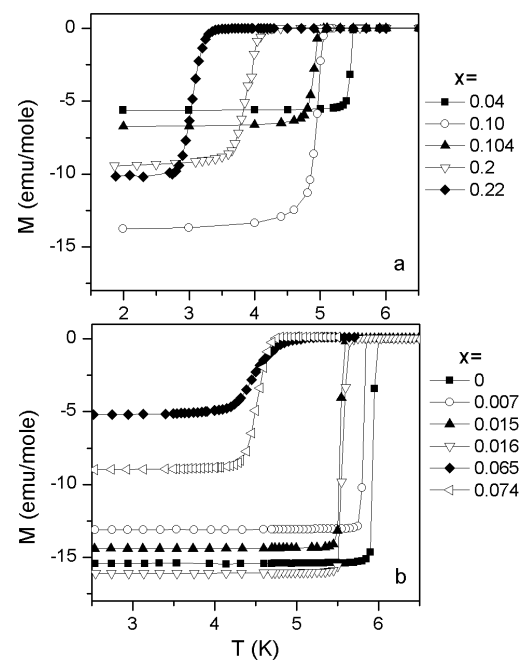


Fig. 1. Temperature dependences of zero-field cooled magnetization at $H = 5$ – 20 Oe of “nonmagnetic” (a) and “magnetic” (b) (see text) $\text{Lu}_x\text{Zr}_{1-x}\text{B}_{12}$ crystals.

*corresponding author; e-mail: azarevich@lt.gpi.ru

2. Results and discussion

The single crystals of $\text{Lu}_x\text{Zr}_{1-x}\text{B}_{12}$ solid solutions were grown by vertical crucible-free inductive floating zone melting in an inert gas atmosphere. To verify both the quality of the samples and the Lu content, x-ray diffraction, Laue backscattering patterns, and microanalysis techniques were used. For all $\text{Lu}_x\text{Zr}_{1-x}\text{B}_{12}$ single crystals the Lu/Zr ratio was estimated using a scanning electron microscope equipped with an energy dispersion microprobe system (JEOL JXA-8200 EPMA), see also [7] for details.

Studies of resistivity, heat capacity and magnetization of high-quality single crystals of $\text{Lu}_x\text{Zr}_{1-x}\text{B}_{12}$ with $x < 35\%$ and $x \geq 90\%$ were carried out at temperatures between 0.06 and 300 K, and in magnetic fields up to 90 kOe ($\mathbf{H} \parallel (001)$). For example, Fig.1 shows the temperature dependences of zero-field cooled magnetization $M(T)$ at $H = 5 \div 20$ Oe in the vicinity of T_c for crystals with $x < 35\%$.

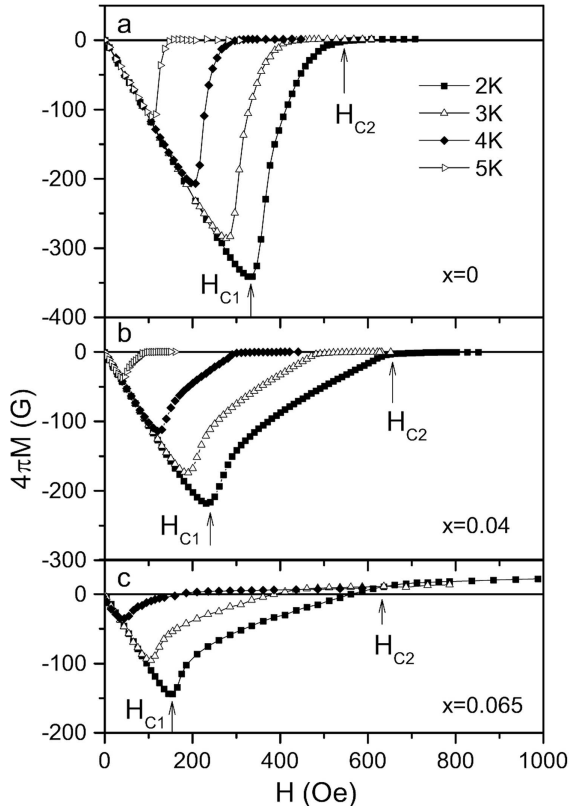


Fig. 2. Magnetic field $M(H, T_0)$ dependences of $\text{Lu}_x\text{Zr}_{1-x}\text{B}_{12}$ with $x = 0$ (a), 0.04 (b) and 0.065 (c). Critical fields H_{c1} and H_{c2} are indicated by arrows.

Figure 2 presents the magnetic field $M(H)$ curves recorded at temperatures $T_0 < T_c$ for lutetium concentrations $x = 0, 0.04$ and 0.065 (see panels a-c, correspondingly). The $M(H)$ dependences are linear for H below the first critical field ($H < H_{c1} \sim 100 \div 400$ Oe) and may be attributed to the total Meissner effect. Additionally, the second critical field H_{c2} is detected from

these dependences for all crystals under investigation. Based on these results, shown e.g. in Figs. 1 and 2, we present on Fig. 3 the concentration dependence $T_c(x)$ (insert) and the $H-T$ phase diagram of $\text{Lu}_x\text{Zr}_{1-x}\text{B}_{12}$ solid solutions with a wide range of Lu content. The estimated Ginzburg-Landau parameter κ of these compounds varies between 0.9 ($x = 0$) and 4 ($x = 0.22$).

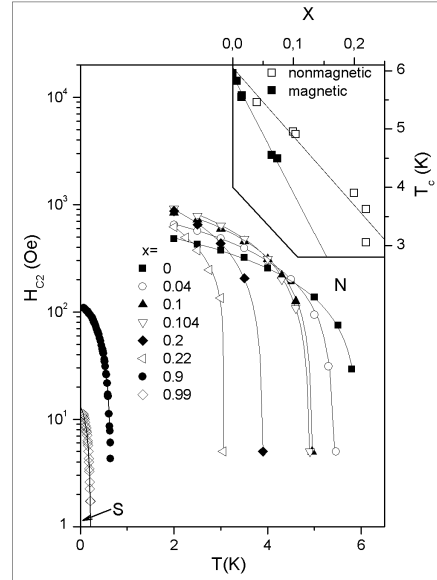


Fig. 3. Suppression of superconductivity $T_c(x)$ (see insert) and the $H-T$ phase diagram of $\text{Lu}_x\text{Zr}_{1-x}\text{B}_{12}$ solid solutions (nonmagnetic samples). S and N mark the superconducting and normal states, correspondingly.

It is worth noting that two types of $M(H)$ behavior were observed in this study for solid solutions with a low concentration of lutetium in the paramagnetic state just above the critical field H_{c2} . For the first set of $\text{Lu}_x\text{Zr}_{1-x}\text{B}_{12}$ crystals only a very small paramagnetic signal was detected (see, for example, Figs.2a and 2b). On the contrary, for other samples with a similar Lu concentration the magnetization demonstrates a rather strong increase above H_{c2} (see Fig.2c) which has been interpreted (see [7] for details) in terms of an emergence of magnetic moments embedded in the nonmagnetic matrix of $\text{Lu}_x\text{Zr}_{1-x}\text{B}_{12}$. It is worth noting that in our experimental study also attempts were undertaken to measure the field dependence of magnetization of $\text{Lu}_x\text{Zr}_{1-x}\text{B}_{12}$ crystals with the help of a PPMS-9 system. However, the signal from the sample holder which was comparable with the magnetization of samples under investigation did not allowed us to carry out the separation and analysis of contributions in strong magnetic fields. For these magnetic solid solutions an additional magnetic component C_m appears also in the low temperature heat capacity (see e.g. Fig. 4b), and this C_m amplitude increases

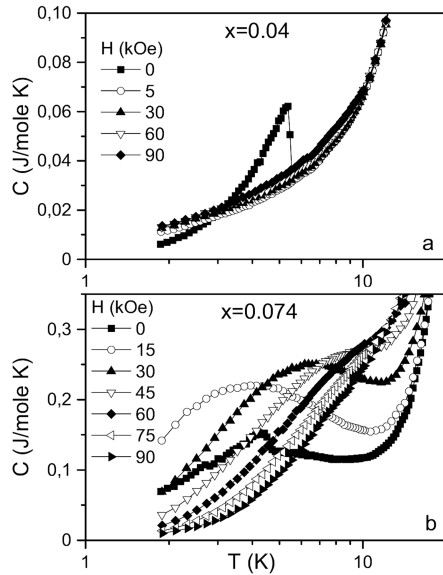


Fig. 4. Temperature dependences of specific heat $C(T, H_0)$ for (a) nonmagnetic $x = 0.04$ and (b) magnetic $x = 0.074$ crystals of $\text{Lu}_x\text{Zr}_{1-x}\text{B}_{12}$ (see also [7] for details).

in external magnetic field. The analysis of $C_m(T, H_0)$ made for the magnetic samples in [7] allows to conclude that the magnetic sites are created in the vicinity of lutetium impurities. In the set of magnetic solid solutions the magnetic contribution was found also in magnetoresistance and ESR (electron spin resonance) studies of $\text{Lu}_x\text{Zr}_{1-x}\text{B}_{12}$ [7]. On the other hand, the C_m contribution is practically negligible for nonmagnetic crystals (see e.g. Fig. 4a).

These two types of $\text{Lu}_x\text{Zr}_{1-x}\text{B}_{12}$ crystals, the “magnetic” ones (see also [7] for details) and the “nonmagnetic” ones, differ also when the suppression rates of superconductivity $T_c(x)$ are compared between each other (see insert in Fig. 3). Indeed, two $T_c(x)$ branches can be evidently distinguished in Fig. 3 with rates of $dT_c/dx = 0.12$ K/at.% of Lu and 0.21 K/at.% of Lu for the nonmagnetic and magnetic crystals, correspondingly.

3. Conclusions

We have studied the suppression of superconductivity in $\text{Lu}_x\text{Zr}_{1-x}\text{B}_{12}$ solid solutions in a wide range of Lu contents ($0 \leq x \leq 1$). It was shown by resistivity, magnetization and heat capacity measurements, that there are two types of $\text{Lu}_x\text{Zr}_{1-x}\text{B}_{12}$ single crystals with a quite different pair-breaking effect. An unusually strong T_c suppression was observed for samples with nanosized magnetic moments which appear in the vicinity of nonmagnetic Lu-ions embedded in the boride matrix. However, it is not clear why the second set of similar $\text{Lu}_x\text{Zr}_{1-x}\text{B}_{12}$ solid solutions (with $x < 0.3$) exhibits a different behavior.

The reason for this difference may lie in the different distribution and structure of the Lu component in the $\text{Lu}_x\text{Zr}_{1-x}\text{B}_{12}$ matrix. To solve this problem, further investigations displaying above all the detailed distribution of the Lu component in these solid solutions (e.g. by SEM - scanning electron microscopy or STM - scanning tunneling microscopy) will be needed. For example, in case of YB_6 superconductor it was shown recently [8] that the local accumulation of single structural defects (e.g. vacancies or yttrium ion displacements) into complexes leads to formation of magnetic moments in the boride lattice which result into a suppression of superconductivity in this compound.

Acknowledgments

This work was supported by RFBR Project No. 15-02-02553a. The measurements were carried out in the Shared Facility Centre of Lebedev Physical Institute of RAS and the Centre of Excellence SAS. K.F. and S.G. acknowledges partial support by Slovak agencies VEGA 2/0032/16 and APVV-0605-14.

References

- [1] J. Nagamatsu, N. Nakagawa, T. Muranaka, Y. Zenitani, J. Akimitsu, *Nature* **410**, 63 (2001).
- [2] R. Lortz, Y. Wang, S. Abe, C. Meingast, Yu.B. Paderno, V. Filippov, A. Junod, *Phys. Rev. B* **72**, 024547 (2005).
- [3] Y. Wang, R. Lortz, Yu.B. Paderno, V. Filippov, S. Abe, U. Tutsch, A. Junod, *Phys. Rev. B* **72**, 024548 (2005).
- [4] J. Teyssier, R. Lortz, A. Petrovic, D. van der Marel, V. Filippov, N. Shitsevalova, *Phys. Rev. B* **78**, 134504 (2008).
- [5] N. Sluchanko, S. Gavrilkin, K. Mitsen, A. Kuznetsov, I. Sannikov, V. Glushkov, S. Demishev, A. Azarevich, A. Bogach, A. Lyashenko, A. Dukhnenko, V. Filipov, S. Gabáni, K. Flachbart, J. Vanacken, G. Zhang, V. Moshchalkov, *J. Supercond. Novel Magn.* **26**, 1663 (2013).
- [6] K. Flachbart, S. Gabáni, K. Gloos, M. Meissner, M. Opel, Yu. Paderno, V. Pavlik, P. Samuely, E. Schuberth, N. Shitsevalova, K. Siemensmeyer, P. Szabo, *J. Low Temp. Phys.* **140**, 339 (2005).
- [7] N. Sluchanko, A. Azarevich, M. Anisimov, A. Bogach, S. Gavrilkin, M. Gilmanov, V. Glushkov, S. Demishev, A. Khoroshilov, A. Dukhnenko, K. Mitsen, N. Shitsevalova, V. Filippov, V. Voronov, K. Flachbart, *Phys. Rev. B* **93**, 085130 (2016).
- [8] N. Sluchanko, V. Glushkov, S. Demishev, A. Azarevich, M. Anisimov, A. Bogach, S. Gavrilkin, K. Mitsen, A. Kuznetsov, I. Sannikov, N. Shitsevalova, V. Filippov, M. Kondrin, K. Flachbart, *Cond. Mat. arXiv:1608.08902v1*.